JOURNAL OF NATURAL PRODUCTS

Note

pubs.acs.org/jnp

Griseusins F and G, Spiro-Naphthoquinones from a Tin Mine Tailings-Derived Alkalophilic *Nocardiopsis* Species

Zhang-Gui Ding,[†] Jiang-Yuan Zhao,[†] Ming-Gang Li,[†] Rong Huang,[†] Qing-Ming Li,[‡] Xiao-Long Cui,[†] Hua-Jie Zhu,*[,‡] and Meng-Liang Wen*[,†]

[†]Key Laboratory for Microbial Resources, Key Laboratory of Medicinal Chemistry for Natural Resources, Ministry of Education, Yunnan Institute of Microbiology, Yunnan University, Kunming, 650091, People's Republic of China

[‡]State Key Laboratory of Phytochemistry and Plant Resources in West China, Kunming Institute of Botany, Chinese Academy of Sciences, Kunming, 650204, People's Republic of China

Supporting Information

ABSTRACT: Griseusins F (**1**) and G (**2**), two 2a-hydro-8a-(2-oxopropyl)-substituted spiro-naphthoquinones with a previously undescribed C_{23} polyketide skeleton, were isolated from a Yunnan tin mine tailings-derived alkalophilic actinomycete, *Nocardiopsis* sp. YIM DT266. Their complete structure assignments with the absolute stereochemistry were elucidated by spectroscopic data, X-ray crystal diffraction, calculation of optical rotation, and CD spectroscopic analysis. Compounds **1** and **2** exhibited strong cytotoxicity (IC_{50} 0.37−0.82 μM) and antibacterial activity (MIC 0.80−1.65 μg/mL) against Gram-positive bacteria, including methicillin-resistant *Staphylococcus aureus* (MRSA) *in vitro*.

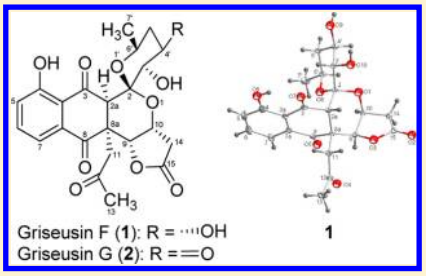

The griseusins, which belong to the family of pyranonaphthoquinones that possess additional heterocyclic rings in the core skeleton of naphtha[2,3-*c*]pyran-5,10-dione,[1,2] are aromatic polyketide antibiotics produced by *Streptomyces griseus* K-63,[3−5] *S. griseus* MJ361-48F3,[6] *Streptomyces.* sp. IFM 11307,[7] actinomycete strain MJ932-SF3,[8] alkaphilic *Nocardiopsis* sp.,[9,10] and *Penicillium* sp.[11] Members of this class exhibit interesting biological activities, such as cytotoxic and antimicrobial activity against methicillin-resistant *Staphylococcus aureus* (MRSA). During our continuing search for new secondary metabolites of Chinese tin mine tailings-derived actinomycetes,[12,13] two unprecedented 2a-hydro-8a-(2-oxopropyl)-substituted spiro-naphthoquinones with a previously undescribed C_{23} polyketide skeleton were isolated from alkalophilic *Nocardiopsis* sp. YIM DT266, namely, griseusin F (**1**) and griseusin G (**2**) (Figure 1). Herein, details are reported regarding the structure elucidation of the two new members of this unique class of natural products, including their absolute stereochemistry and biological activity.

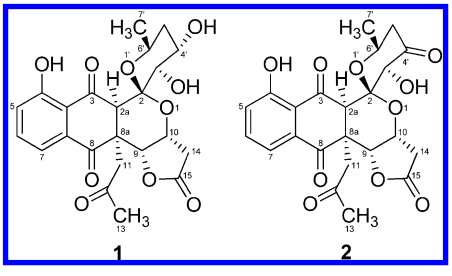

Figure 1. Absolute configuration of griseusins F (**1**) and G (**2**).

Compound **1** was obtained as brown crystals. Its molecular formula was determined to be $C_{23}H_{24}O_{10}$ on the basis of HRMS (ESI+) for a pseudomolecular ion $[M + Na]^+$. ^1H and ^{13}C NMR spectroscopic data of **1** (Table 1) showed resonances for three exchangeable protons, two methyl groups, three methylenes, six methines (five of which are oxymethines), six sp^2 carbons (three protonated), two sp^3 quaternary carbons including one of double oxygenation (δ_C 98.2), three keto carbonyls (δ_C 204.5, 200.5, and 193.7), and one ester/lactone carbonyl (δ_C 174.5). These data accounted for seven out of the 12 degrees of unsaturation calculated from the molecular formula, which suggested that **1** was a pentacyclic compound. Analysis of the $^1H-^1H$ COSY and HMQC-TOCSY spectra of **1** revealed the presence of three discrete $^1H-^1H$ spin systems: H-5/H-6/H-7, H-9/H-10/H_2-14, and H-3′(OH-3′)/H-4′(OH-4′)/H_2-5′/H-6′/H_3-7′ (Figure 2), while H-2a, H_2-11, and H_3-13 were isolated. Comprehensive analysis of the HMBC spectrum of **1** established two main structural fragments, **1a** and **1b** (Figure 2). On the basis of HMBC correlations from H-5, H-7, and OH-4 to C-3a and from H-6 to C-7a, the 1,2,3-trisubstituted phenyl group fusing at positions C-3a/C-7a of fragment **1a** was deduced. An exchangeable proton at δ_H 11.89 in the downfield region of the ^1H NMR spectrum revealed the presence of strong hydrogen bonding, and the HMBC correlations of OH-4 to its adjacent carbons confirmed the assignment of the hydroxyl substitution to C-4. HMBC correlation of H-7 to C-8 indicated the location of carbonyl C-8 and led to assignment of the regio location for H-7. Further HMBC correlations of H-2a to C-3, C-3a, C-8, and C-8a

Received: July 17, 2012
Published: October 24, 2012

Table 1. ^{1}H (500 MHz) and ^{13}C NMR (125 MHz) Data of Compounds 1 and 2

	griseusin F (**1**)			griseusin G (**2**)		
position	δ_C, type	δ_H (J in Hz)	HMBC	δ_C, type	δ_H (J in Hz)	HMBC
2	98.2, C			100.8, C		
2a	53.0, CH	3.46, s	2/2′, 3, 3a, 8, 8a, 11	52.4, CH	3.44, s	2/2′, 3, 3a, 8, 8a, 9, 11, 3′
3	200.5, C			199.6, C		
3a	117.0, C			117.1, C		
4	160.1, C			160.4, C		
5	122.7, CH	7.28, d, (8.1)	3a, 4, 7	122.9, CH	7.30, d, (7.9)	3a, 4, 7
6	137.4, CH	7.74, dd, (8.1, 7.5)	4, 7a	137.6, CH	7.78, dd, (7.9, 7.3)	3a, 4, 7, 7a
7	117.2, CH	7.36, d, (7.5)	3a, 5, 8	117.4, CH	7.39, d, (7.3)	3a, 4, 5, 6, 8
7a	135.0, C			135.0, C		
8	193.7, C			193.9, C		
8a	47.7, C			47.6, C		
9	74.8, CH	5.31, d, (1.8)	2a, 8, 8a, 10	74.5, CH	5.32, d, (1.8)	2a, 8, 8a, 10, 11
10	66.6, CH	4.42, dd, (4.3, 1.8)	15	67.4, CH	4.51, m	9, 15
11	47.1, CH_2	3.08, d, (16.5)	2a, 8, 8a, 9, 12	47.1, CH_2	3.13, d, (17.1)	2a, 8, 8a, 9, 12
		2.86, d, (16.5)	2a, 8, 8a, 9, 12		2.94, d, (17.1)	2a, 8, 8a, 9, 12
12	204.5, C			204.5, C		
13	31.0, CH_3	1.97, s	11, 12	30.9, CH_3	1.98, s	8a, 11, 12
14	37.5, CH_2	3.20, dd, (17.1, 4.3)		37.5, CH_2	3.20, dd, (17.1, 4.0)	15
		2.41, d, (17.1)	9, 10, 15		2.33, d, (17.1)	9, 10, 15
15	174.5, C			174.1, C		
3′	72.6, CH	3.00, dd, (9.2, 6.7)	2/2′, 2a, 8a, 4′	74.7, CH	4.07, d, (6.7)	2/2′, 2a, 4′
4′	66.8, CH	3.59, m[a]	2a	203.8, C		
5′	40.8, CH_2	1.71, m	3′, 4′	46.4, CH_2	2.30, m	3′, 4′, 6′, 7′
		1.68, m	3′, 4′		2.22, m	3′, 4′
6′	65.7, CH	3.61, m[a]	2a	67.4, CH	3.87, m	
7′	19.3, CH_3	0.58, d, (6.1)	5′, 6′	19.7, CH_3	0.74, d, (6.1)	4′, 5′, 6′
OH-4		11.89, s	3a, 4, 5		11.85, s	3a, 4, 5
OH-3′		4.90, d, (6.7)	2/2′, 3′, 4′		5.48, d, (6.7)	2/2′, 3′, 4′
OH-4′		4.62, d, (4.9)	5′			

[a]The signals of H-4′ and H-6′ overlap.

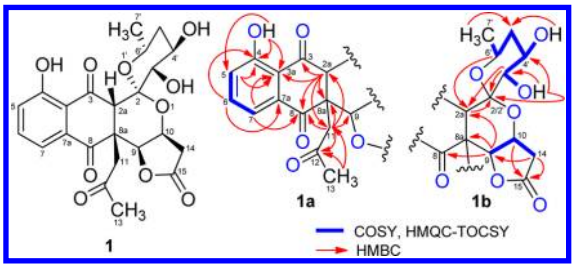

Figure 2. Structure of **1**. Selected COSY, HMQC-TOCSY, and HMBC correlations of fragments **1a** and **1b**.

suggested a 2,3-disubstituted dihydrojuglone moiety for fragment **1a**, in which the C-2a/C-8a bond was saturated. A 2-oxopropyl group at C-8a was supported by HMBC cross-peaks from H_2-11 to C-2a, C-8, C-8a, and C-9. In fragment **1b**, the HMBC correlations of H-2a, H-3′, and OH-3′ with the quaternary ketal C-2/2′, H-4′ and H-6′ with C-2a, and H-9 with C-2a and C-8a enabled the construction of a 1,7-dioxaspiro[5.5]undecane ring system. A γ-lactone ring was fused into the pyran moiety at positions C-9/C-10 as evidenced by the $^{2}J_{C,H}$ couplings (H-9/C-8a) and $^{3}J_{C,H}$ couplings (H-9/C-8, H-10/C-15, and H_2-14/C-9) observed in the HMBC spectrum. Therefore, the planar structure of **1** was tentatively assigned as depicted in Figure 2.

The relative configuration of **1** was determined by analysis of its ^{1}H NMR and 2D-NOESY correlations. H-2a and C-8a/C-11 in *syn* orientation was evidenced by an NOE interaction between H-2a and H_2-11. The NOESY correlation of H-9 with H-10 indicated the *cis* attachment of the γ-lactone ring (Figure 3). A coupling constant of 9.2 Hz for $^{3}J_{H\text{-}3',H\text{-}4'}$ strongly

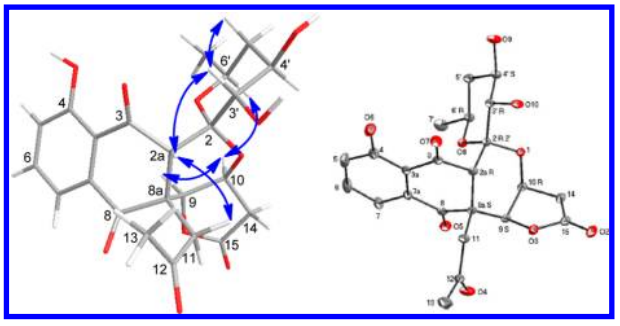

Figure 3. Selected NOESY correlations (left) and ORTEP representation (right) of **1**.

suggested a diaxial arrangement of H-3′ and H-4′. Furthermore, the axial position of H-3′ was confirmed by an NOE between H-3′ and H_{ax}-5′. Finally, the relative configuration of **1** was confirmed by single-crystal X-ray diffraction analysis (Figure 3).[14]

The absolute configuration of the eight stereogenic centers in **1** was assigned by comparing the computed optical rotation (OR) with the experimental OR through the use of methods reported by other investigators,[15−17] as well as DFT methods previously employed by this group.[18] The computed OR for **1**

dx.doi.org/10.1021/np3004936 | J. Nat. Prod. 2012, 75, 1994−1998

was −145.1 at the B3LYP/6-311++G(2d,p) level. The recorded OR for **1** was +109.0. The absolute OR for **1** (109.0) is closer to the computed value (−145.1); however, the OR signs (negative vs positive) contradict each other. The proposed structure of **1** (Figure 2) must therefore represent the enantiomer of the naturally occurring compound. Accordingly, the absolute configurations of the eight stereogenic centers in **1** were determined to be 2*R*, 2a*S*, 8a*S*, 9*R*, 10*R*, 3′*R*, 4′*S*, and 6′*R* (Figure 1).

The molecular weight of compound **2** was 2 Da lower than that of **1**, as determined by HRMS (ESI+) for a pseudomolecular ion $[M + Na]^+$. The molecular formula of $C_{23}H_{22}O_{10}$ for **2** suggested that it is an analogue of **1** after dehydrogenation. Consistent with this inference, ^1H and ^{13}C NMR data of **2** (Table 1) were very similar to those of **1** except that one oxymethine carbon signal (δ_C 66.8, C-4′) in **1** was replaced by a signal for a keto carbonyl carbon in **2** (δ_C 203.8, C-4′). The new keto group was located at C-4′, as assessed by the HMBC correlations of H-3′, OH-3′, H_2-5′, and H_3-7′ with C-4′. Further HMBC correlations (Figure 4) confirmed the structure **2** as depicted.

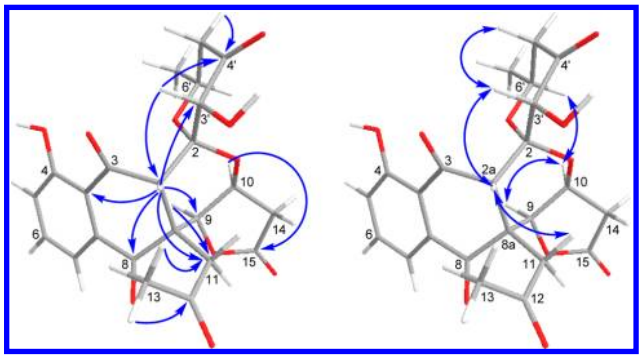

Figure 4. Selected HMBC (left) and NOESY (right) correlations of **2**.

The similar NOESY correlations of **1** and **2** (Figures 3 and 4) revealed the same stereostructure for both compounds. The absolute configuration of **2** was assigned by comparison of the CD spectrum of **2** with that of **1** (Figure 5), as well as by comparison of the experimental and calculated OR values of **2** (experimental, +128.5; calculated, −157.3). Considering that both compounds are produced by the same strain (YIM DT266) of *Nocardiopsis* sp. and exhibited almost identical CD curves, the absolute configurations of the seven stereogenic centers in **2** were determined to be 2*R*, 2a*S*, 8a*S*, 9*R*, 10*R*, 3′*R*, and 6′*R* (Figure 1).

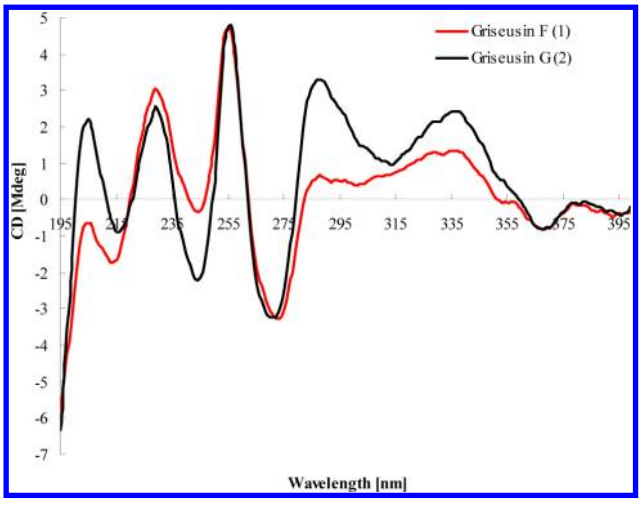

Figure 5. CD spectra of **1** and **2**.

As noted above, griseusins F (**1**) and G (**2**) are new members of the rare 2a,8a-disubstituted class of natural griseusins. They are characterized by unprecedented 2a-hydro-8a-(2-oxopropyl) structural variations; they are also the first metabolites possessing a novel C_{23} polyketide skeleton within this class of compounds. Compared with the closely related pyranonaphthoquinones, such as the recently isolated *epi*-4′-deacetyl-(−)-griseusin A (**3**),[9] 4′-dehydrodeacetyl-(−)-griseusin A (**4**),[9] 2a,8a-epoxy-*epi*-deacetyl-(+)-griseusin B (**5**),[9] (−)-griseusin D (**6**),[10] and (+)-griseusin E (**7**)[7] (Figure 6), **1** and **2** are uniquely

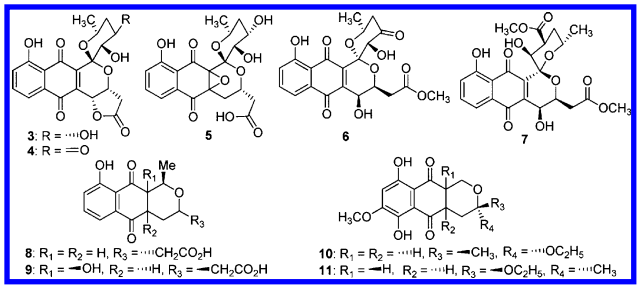

Figure 6. Related microbial metabolites.

modified. Specifically, the C-2a/C-8a double bond in **3**, **4**, **6**, and **7** has been opened by the *cis* addition of H/2-oxopropyl to create two new sp^3 chiral centers in **1** and **2**, which also differ from the epoxy substitution at C-2a/C-8a in **5**. Moreover, the H/2-oxopropyl substitution at C-2a/C-8a in **1** and **2** results in CD spectra and/or signs of OR that are significantly different from those of **3**−**7**. This is the first report to establish the absolute configurations of new chiral centers at C-2a and C-8a in **1** by single-crystal X-ray diffraction analysis and calculation of the OR, whereas the counterparts in the related microbial metabolites, tetrahydrokalafungin (**8**),[19] nanaomycin B (**9**),[20] and the dihydrofusarubin ethyl acetals (**10**, **11**)[21−23] (Figure 6), have yet to be determined.

1 and **2**, like griseusins A and B, are assumed to be formed by the polyketide biosynthesis pathway.[24] It can also be speculated that reduction of the polyketide backbone at C-2a and C-8a requires additional enzymatic reduction of the polyketide skeleton.

Cytotoxicity and Antibacterial Activity. **1** and **2** exhibited highly cytotoxic activity against B16, MDA-MB-435S, CFPAC-1, ACHN, and HCT-116 human cancer cell lines (Table 2). Antibacterial activity is reported in Table 3.

EXPERIMENTAL SECTION

General Experimental Procedures. Thin-layer chromatography (TLC) and silica gel column chromatography were performed using Nanodurasil-20 UV_{254} plates (Macherey-Nagel & Co) and ZX-3 silica gel (Qindao Haiyang Chemicals), respectively. Preparative HPLC was carried out using a Waters SunFire reversed-phase (C_{18}, 10 μm, 250 × 19 mm, l × i.d.) column connected to a Waters 1525 binary pump and monitored by a Waters photodiode array detector. UV and IR spectra were measured on a Shimadzu 2401PC UV/vis spectrometer and a Bruker Tensor27 FT/IR spectrometer, respectively. Optical rotations were recorded using a Jasco P-1020 polarimeter. CD spectra were recorded on a Chirascan circular dichroism spectrometer. High-resolution mass spectrometric data were obtained from an Agilent

dx.doi.org/10.1021/np3004936 | *J. Nat. Prod.* 2012, 75, 1994−1998

Table 2. Inhibition, IC_{50} (μM)[a], of Human Cancer Cell Lines by Griseusins F (1) and G (2)

cancer cell line[b]	IC_{50} (μM) griseusin F (1)	griseusin G (2)	cisplatin
B16	0.43	0.37	0.31
MDA-MB-435S	0.82	0.69	0.78
CFPAC-1	0.64	0.42	0.48
ACHN	0.55	0.46	0.33
HCT-116	0.70	0.58	0.27

[a]Dose required to inhibit growth to 50% of the untreated cells. [b]B16 = melanoma; MDA-MB-435S = breast carcinoma; CFPAC-1 = pancreatic cancer; ACHN = renal carcinoma; HCT-116 = colon cancer.

Table 3. Antibacterial Activity of Griseusins F (1) and G (2)

strain	average MIC (μg/mL) griseusin F (1)	griseusin G (2)	ciprofloxacin
Staphylococcus aureus ATCC 29213	0.91	0.80	0.28
Micrococcus luteus	1.27	1.47	1.19
Bacillus subtilis	1.65	1.33	0.64

1100 HPLC/TOF system. ^{1}H, ^{13}C, and 2D NMR experiments were acquired on a Bruker DRX-500 MHz spectrometer. The NMR chemical shifts (ppm) were referenced to the solvent peaks at δ_H 2.50 and δ_C 39.5 (residual DMSO) for samples in DMSO-d_6.

Strain and Cultivation. *Nocardiopsis* sp. (YIM DT266) was isolated from an alkaline soil sample (pH 10) collected from the Datun tin mine tailings area (103°18′36″ E, 23°22′12″ N), Yunnan, PR China. The soil in this area is contaminated with high contents of metals (including 1.4 × 105 mg kg^{-1} iron, 2.9 × 103 mg kg^{-1} tin, 1.8 × 103 mg kg^{-1} arsenic, 1.2 × 103 mg kg^{-1} copper, and 4.4 × 102 mg kg^{-1} lead). It was classified according to 16S rRNA analysis with 97.3% identity (Genbank deposit no. GU138159). A voucher specimen is deposited at Yunnan Institute of Microbiology, Yunnan University, with the code YIM DT266. Strain YIM DT266 was cultured in 2000 agar plates composed of 10 g/L glucose, 5 g/L peptone, 5 g/L yeast extract, 1 g/L K_2HPO_4, 0.2 g/L $MgSO_4{\cdot}7H_2O$, 18 g/L Na_2CO_3, and 15 g/L agar in distilled H_2O, pH 12. Sodium carbonate was sterilized separately and then added to the medium. The plates were incubated at 28 °C for 28 days.

Computational Method. The conformational search was performed by Amber force field via the HyperChem package. The geometries with a relative energy of 0−5 kcal/mol were used in optimizations at the B3LYP/6-31G(d) level. Only the geometries with an energy of 0−2.5 kcal/mol were used in optical rotations at the B3LYP/6-311++G(2d,p) level. Boltzmann statistics used whole conformational OR sums. The computed ORs for griseusins F (1) and G (2) were −145.1 and −157.3, respectively.

Extraction, Isolation, and Purification. The cultured plates were extracted with methanol. The extract was concentrated under reduced pressure, and the aqueous residue was extracted with EtOAc. The EtOAc fraction was first chromatographed on a silica gel flash chromatograph eluted with $CHCl_3$/MeOH (9:1) and then fractionated using Sephadex LH-20 eluted with MeOH. Further purification was achieved by preparative reversed-phase HPLC using an isocratic elution of MeOH/H_2O (6:4) to obtain griseusin F (**1**, yield 0.87 mg L^{-1}, t_R 4.9 min) and griseusin G (**2**, yield 0.64 mg L^{-1}, t_R 5.7 min). Finally, slow recrystallization of griseusin F (**1**) from MeOH/H_2O (95:5) furnished single crystals suitable for X-ray experiment.

Griseusin F (1): brown crystal; mp >300 °C; $[\alpha]^{20}_D$ +109.0 (*c* 0.0014, MeOH); UV (MeOH) λ_{max} (log ε) 201.0 (3.9), 232.0 (4.0), 353.0 (3.4); CD (MeOH) λ ($\Delta\varepsilon$) 204 (−0.64), 213 (−1.75), 229 (+3.03), 244 (−0.33), 255 (+4.72), 273 (−3.29), 288 (+0.66), 336 (+1.33), 368 (−0.83), 379 (−0.11); IR (KBr) ν_{max} 3495.5, 3476.4, 2951.3, 2924.7, 2854.0, 1773.4, 1725.5, 1697.9, 1641.4, 1455.7 cm^{-1}; HRMS (ESI) *m/z* calcd for $[C_{23}H_{24}O_{10} + Na]^+$ 483.1262 [M + Na]$^+$, found 483.1255; *m/z* calcd for $[2 \times C_{23}H_{24}O_{10} + Na]^+$ 943.2631 [2 M + Na]$^+$, found 943.2623; *m/z* calcd for $[C_{23}H_{24}O_{10} - H]^-$ 459.1297 [M − H]$^-$, found 459.1296.

Griseusin G (2): brown crystal; mp >300 °C; $[\alpha]^{20}_D$ +128.5 (*c* 0.0020, MeOH); UV (MeOH) λ_{max} (log ε) 201.5 (4.0), 231.5 (4.2), 353.0 (3.6); CD (MeOH) λ ($\Delta\varepsilon$) 205 (+2.22), 216 (−0.90), 229 (+2.55), 244 (−2.24), 256 (+4.79), 271 (−3.24), 288 (+3.30), 313 (+0.96), 336 (+2.43), 368 (−0.83), 383 (−0.04); IR (KBr) ν_{max} 3442.3, 2976.1, 2933.1, 2855.4, 1795.0, 1726.1, 1701.9, 1641.0, 1455.4 cm^{-1}; HRMS (ESI) *m/z* calcd for $[C_{23}H_{22}O_{10} + Na]^+$ 481.1105 [M + Na]$^+$, found 481.1101; *m/z* calcd for $2 \times [C_{23}H_{22}O_{10} + Na]^+$ 939.2318 [2 M + Na]$^+$, found 939.2317; *m/z* calcd for $[C_{23}H_{22}O_{10} - H]^-$ 457.1140 [M − H]$^-$, found 457.1137.

Biological Assays. The cytotoxic effects on cancer cell lines (B16, MDA-MB-435S, CFPAC-1, ACHN, and HCT-116 cells, which were obtained from Kunming Medical University) were determined by MTT assay.[25] Briefly, 100 μL of each cell line (5 × 10^4 cells mL^{-1}) was seeded in 96-well microplates and incubated at 37 °C for 24 h. Then, 100 μL of various concentrations of the test chemical in DMSO was added. Cisplatin was used as a positive control. After 24, 48, and 72 h, the cells were stained with MTT. The optical density of each well was measured at 492 nm compared to the negative control. The data obtained were presented graphically by plotting the test chemical concentrations versus the percent cell viability, where the concentration causing cell death by 50% was determined as the half-maximal inhibitory concentration (IC_{50}). The MICs for antibacterial activity were determined by agar well diffusion assay using tested bacteria (*Staphylococcus aureus* ATCC 29213, *Micrococcus luteus*, and *Bacillus subtilis*).[26] The MICs were read in μg/mL after overnight incubation at 28 °C.

■ ASSOCIATED CONTENT

Supporting Information

NMR data of **1** and **2**, ^{1}H and ^{13}C NMR, 2D NMR (HSQC, COSY, HMQC-TOCSY, HMBC, and NOESY), HRESI MS, CD, IR, and UV spectra of **1** and **2**, and crystallographic data of **1**. This material is available free of charge via the Internet at http://pubs.acs.org.

■ AUTHOR INFORMATION

Corresponding Author

*E-mail: mlwen@ynu.edu.cn; hjzhu@mail.kib.ac.cn.

Notes

The authors declare no competing financial interest.

■ ACKNOWLEDGMENTS

This work was supported by National Natural Science Foundation of China (21102126, 21162039, 31060011), National Key Technologies R&D Program (2010GB2F300435, 2011BAE06B04-17), 973 Program (2009CB522300), Yunnan Provincial Science and Technology Department (W8011303), and Yunnan University (2011YB03, 2009C17Q).

■ REFERENCES

(1) Brimble, M. A.; Duncalf, L. J.; Nairn, M. R. *Nat. Prod. Rep.* **1999**, *16*, 267−281.

(2) Sperry, J.; Bachu, P.; Brimble, M. A. *Nat. Prod. Rep.* **2008**, *25*, 376−400.

(3) Tsuji, N.; Kobayashi, M.; Wakisaka, Y.; Kawamura, Y.; Mayama, M.; Matsumoto, K. *J. Antibiot.* **1976**, *29*, 7−9.

(4) Tsuji, N.; Kobayashi, M.; Terui, Y.; Tori, K. *Tetrahedron* **1976**, *32*, 2207−2210.

(5) Tsuji, N.; Kamigauchi, T.; Nakai, H.; Shiro, M. *Tetrahedron Lett.* **1983**, *24*, 389−390.
(6) Maruyama, M.; Nishida, C.; Takahashi, Y.; Naganawa, H.; Hamada, M.; Takeuchi, T. *J. Antibiot.* **1994**, *47*, 952−954.
(7) Abdelfattah, M. S.; Kazufumi, T.; Ishibashi, M. *J. Antibiot.* **2011**, *64*, 729−734.
(8) Igarashi, M.; Chen, W.; Tsuchida, T.; Umekita, M.; Sawa, T.; Naganawa, H.; Hamada, M.; Takeuchi, T. *J. Antibiot.* **1995**, *48*, 1502−1505.
(9) He, J.; Roemer, E.; Lange, C.; Huang, X.; Maier, A.; Kelter, G.; Jiang, Y.; Xu, L. H.; Menzel, K. D.; Grabley, S.; Fiebig, H. H.; Jiang, C. L.; Sattler, I. *J. Med. Chem.* **2007**, *50*, 5168−5175.
(10) Li, Y. Q.; Li, M. G.; Li, W.; Zhao, J. Y.; Ding, Z. G.; Cui, X. L.; Wen, M. L. *J. Antibiot.* **2007**, *60*, 757−761.
(11) Li, X.; Zheng, Y.; Sattler, I.; Lin, W. *Arch. Pharm. Res.* **2006**, *29*, 942−945.
(12) Ding, Z. G.; Li, M. G.; Zhao, J. Y.; Ren, J.; Huang, R.; Xie, M. J.; Cui, X. L.; Zhu, H. J.; Wen, M. L. *Chem.−Eur. J.* **2010**, *16*, 3902−3905.
(13) Ding, Z. G.; Li, M. G.; Ren, J.; Zhao, J. Y.; Huang, R.; Wang, Q. Z.; Cui, X. L.; Zhu, H. J.; Wen, M. L. *Org. Biomol. Chem.* **2011**, *9*, 2771−2776.
(14) X-ray measurements were made on a SMART CCD area detector with graphite-monochromated Mo Kα radiation (λ = 0.71073 Å). Compound **1** (MF $C_{23}H_{24}O_{10}$, M_r 460.43): crystal dimensions 0.30 × 0.21 × 0.14 mm; orthorhombic space group $P2_12_12_1$, a = 9.3981(15) Å, b = 9.5761(15) Å, c = 23.701(4) Å; V = 2133.0(6) Å^3; Z = 4; ρ_{calcd} = 1.434 mg m^{-3}; μ = 0.113 mm^{-1}; T = 298(2) K; $2\theta_{max}$ = 56.7°; 13 793 measured reflections; 5005 independent reflections (R_{int} = 0.0556); 303 parameters refined; R = 0.0490 (for 5005 reflections with $I > 2.00\sigma(I)$); R_w = 0.0787; max/min residual peaks in the final difference map 0.186/−0.188 e Å^{-3}. Crystallographic data (excluding structure factors) for the compound **1** in this paper have been deposited with the Cambridge Crystallographic Data Centre as supplementary publication no. CCDC 797552. Copies of the data can be obtained, free of charge, on application to CCDC, 12 Union Road, Cambridge CB2 1EZ, UK (fax: +44-(0)1223-336033 or e-mail: deposit@ccdc.cam.ac.uk).
(15) Wipf, P.; Spencer, S. R. *J. Am. Chem. Soc.* **2005**, *127*, 225−235.
(16) Zuber, G.; Goldsmith, M. R.; Hopkins, T. D.; Beratan, D. N.; Wipf, P. *Org. Lett.* **2005**, *7*, 5269−5272.
(17) Yang, X. W.; Ding, Y.; Li, X. C.; Ferreira, D.; Shen, Y. H.; Li, S. M.; Wang, N.; Zhang, W. D. *Chem. Commun.* **2009**, 3771−3773.
(18) Ren, J.; Jiang, J. X.; Li, L. B.; Liao, T. G.; Tian, R. R.; Chen, X. L.; Jiang, S. P.; Pittman, C. U., Jr.; Zhu, H. J. *Eur. J. Org. Chem.* **2009**, 3987−3991.
(19) Kakinuma, S.; Ikeda, H.; Takada, Y.; Tanaka, H.; Hopwood, D. A.; Õmura, S. *J. Antibiot.* **1995**, *48*, 484−487.
(20) Tanaka, H.; Koyama, Y.; Nagai, T.; Marumo, H.; Õmura, S. *J. Antibiot.* **1975**, *28*, 868−875.
(21) Kurobane, I.; Vining, L. C.; McInnes, A. G.; Gerber, N. N. *J. Antibiot.* **1980**, *33*, 1376−1379.
(22) Gerber, N. N.; Ammar, M. S. *J. Antibiot.* **1979**, *32*, 685−688.
(23) Barbier, M.; Devys, M.; Parisot, D. *Can. J. Chem.* **1988**, *66*, 2803−2804.
(24) Yu, T. W.; Bibb, M. J.; Revill, W. P.; Hopwood, D. A. *J. Bacteriol.* **1994**, *176*, 2627−2634.
(25) Anke, H.; Bergendorff, O.; Sterner, O. *Food Chem. Toxicol.* **1989**, *27*, 393−397.
(26) Schoettler, S.; Bascope, M.; Sterner, O.; Anke, T. *Z. Naturforsch. C* **2006**, *61*, 309−314.